Coexistence of inertial competitors in chaotic flows

I.J. Benczik[1], G. Károlyi[2], I. Scheuring[3], and T. Tél[4]
[1] *Max Planck Institute for the Physics of Complex Systems, Nöthnitzer Str. 38, 01187 Dresden, Germany,*
[2] *Center for Applied Mathematics and Computational Physics, and Department of Structural Mechanics, Budapest University of Technology and Economics, Műegyetem rkp. 3, H-1111 Budapest, Hungary,*
[3] *Department of Plant Taxonomy and Ecology, and Research Group of Ecology and Theoretical Biology, HAS and Eötvös University, Pázmány P. s. 1/c, 1117 Budapest, Hungary*
[4] *Institute for Theoretical Physics, Eötvös University, P.O. Box 32, H-1518 Budapest, Hungary*
(Dated: October 26, 2005)

We investigate the dynamics of inertial particles immersed in open chaotic flows. We consider the generic problem of competition between different species, e.g plankton populations in oceans. The strong influence from inertial effects is shown to result in the persistence of different species even in cases when the passively advected species cannot coexist. Multi-species coexistence in the ocean can be explained by the fact that the unstable manifold is different for each advected competitor of different size.

PACS numbers: PACS: 87.23.Cc, 47.52.+j, 47.54,Fj, 47.55.Kf

I. INTRODUCTION

The paradox of plankton is a classical problem of ecology. It is well known [1] that in most natural habitats numerous competing species can coexist, while generally only few resources limit these communities. In turn, classical theoretical and experimental studies [2, 3] predict competitive exclusion of all but the most perfectly adopted species for each limiting factor in homogeneous environment. The most frequently discussed example of such ecosystems are phytoplankton communities where hundreds of species can coexist in one cubic meter of ocean, while the number of limiting resources is on the order of ten [1]. To explain the biodiversity present in natural communities many solutions arose based on different mechanisms like spatial or temporal heterogeneity of the environment, predation, disturbance, or coevolution of the competitors [4, 5]. However, to determine which mechanisms are responsible for the coexistence of competitors in a given community is still a matter of vivid debate among ecologists [4, 5].

For phytoplankton communities a so-called "hydrodynamical solution" has been suggested recently [6–9]. This is based on spatial heterogeneities appearing in a stirred, imperfectly mixed environment. The fate of the plankton species is strongly influenced by advection. Stable coexistence has been shown in environments where mixing is imperfect. Species competing for the same resource, advected by an open chaotic flow are accumulating along the unstable manifold of a chaotic set. The unstable manifold is a filamental fractal. Therefore, the less abundant a species becomes, the finer filaments become resolved, hence it has largely increased surface to access resources. The fractal catalyst [10, 11] will increase the production of the weaker species, therefore they can survive and coexist with the stronger one.

In this work we revisit the "hydrodynamical solution of the plankton paradox". The emphasis will be on the changes that inertial effects introduce in the competition dynamics. Interest has recently increased in this kind of "activity" [12–29]. In what follows we use the word *active* in the sense that the particle has finite size and some inertia, and we call *passive* an ideal, pointlike tracer. It has been shown both theoretically and experimentally that the presence of a particle with non-zero size modifies the flow locally and, therefore, the motion of such particle differs [30–32] from that of an ideal passive tracer, which simply follows the local velocity of the flow. Inertial effects can have strong influence on the advection dynamics, ranging from a slight modification to a complete qualitative change of the behaviour as a function of the parameters.

The plankton consist of a huge variety of aquatic organisms, comprising from microplankton about $10\mu m$ in size, to individuals with sizes about $200\mu m$. Their density, in general, is slightly greater than the water's density [33]. For each size and density parameter pair there exists a slightly shifted copy of the unstable manifold along which a species can live. In this way, in principle, as many species can coexist as many different sizes they have.

Finally we mention that the plankton paradox serves only as a motivation, the work constitutes a comprehensive study which incorporate all the parameter regimes where inertial effects has to be taken into account.

The paper is organized as follows. First we introduce the problem of competition in chaotic flows, presenting earlier findings regarding the coexistence of ideal pointlike competitors. In Sec. III we describe the dynamics of inertial tracers which have small but finite size and inertia, along with enumerating the principal inertial effects which appear in a chaotic advection. Sec. IV contains the new results, it describes the competition of species when inertia is superimposed on the advection dynamics. In the last Section the results are summarized and their application to real aquatic systems is discussed.

II. COEXISTENCE OF PASSIVE SPECIES

It has been shown that hydrodynamical phenomena play a keystone role in the population dynamics of passively advected species living in aquatic ecosystems. The main idea is that small scale spatial heterogeneities generated by chaotic advection can lead to coexistence. In this section we recall briefly the basic arguments of these studies [6–9].

In aquatic systems of large extension, on the time scales characteristic to the life cycle of microorganisms, the hydrodynamical flows are locally open, i.e. there is a net current flowing through the region of observation. Most trajectories are unbounded and particles escape the observation region in a finite time. It became clear in the past decade that the motion of passive tracers advected by open hydrodynamical flows is typically chaotic even for simple time-dependent flows, which are not turbulent. Studies of the advection dynamics in chaotic flows have shown that passive particles accumulate on a fractal set, on the unstable manifold of the chaotic invariant set. Recent studies of chemical reactions superimposed on such flows revealed that chemical activity is concentrated along these fractal filaments, and the reaction reaches a steady state [9–11].

A kinetic differential equation was derived for an autocatalytic reaction (or reproduction in biological terms) of type $A + B \to 2B$ in two–dimensional open chaotic flows. Particles participating in the reaction cover the filaments of the unstable manifold with a finite coverage width. The dynamics of the individual number N_B is governed by the equation [9–11]:

$$\frac{dN_B}{dt} = -\kappa N_B + q\,(2-D)\,v_B N_B^{-\beta}, \qquad \text{where} \qquad \beta = \frac{D-1}{2-D} > 0. \tag{1}$$

The first term on the right hand side describes the exponential decay of the species with decay rate κ due to the escape from the chaotic set. The next term is the production term which contains the velocity v_B of the reaction front. Constant q contains geometrical details of the flow. This nontrivial, singular scaling with power $-\beta$ results in a singular enhancement of the productivity associated with the reaction as compared to the productivity in non–chaotic flows. Power $-\beta$ is related in a well–defined way to the fractal dimension of the unstable manifold D. Because the perimeter of the fractal filaments diverges with refining resolution, the unstable manifold acts as a dynamical fractal catalyst. When there is only a small amount of B in the mixing region, reaction is speeded up due to the negative exponent in the second term. If the reactant B is in abundance in the mixing region, the first term will dominate, and outflow speeds up. The balance of these two terms results in a stable steady state with constant production. It has been shown that a similar type of equation remains valid for autocatalytic reactions in non-periodically time-dependent flows, in three-dimensional flows, and also for inertial tracers [9, 29].

Kinetic models of replication and competition: $A + B \to 2B$, $A + C \to 2C$ (with A as the limiting resource for which competition takes place) show that stable coexistence of the species is possible in open chaotic flows for several parameter values [6–8]. The parameter characterising the fitness of the species is usually taken as the ratio γ/d between the reproduction and mortality rates of the species. Species with lower γ/d ratio will be outcompeted in well mixed environment [34]. However, in chaotic flows the dynamical fractal catalyst influences the fate of the populations. The mathematical model describing the mechanisms maintaining coexistence in such hydrodynamical systems [8], consist of two coupled population dynamical processes evolving on a fractal support. The total number of species B and C, $N = N_B + N_C$ follows the equation:

$$\frac{dN}{dt} = -\kappa N + q\,(2-D)\,(p_B\,v_B + p_C\,v_C)\,N^{-\beta}. \tag{2}$$

where v_B and v_C are the reaction front velocities corresponding to the two species. Since the complexity of the chaotic dynamics requires to introduce probabilistic concepts, Eq.(2) contains the probability p_B (p_C) of finding species B (C) on the outer boundary of the fractal filaments. The differential equation for the number N_i of individuals of the two species $i = B, C$ has been derived as:

$$\frac{dN_i}{dt} = -\kappa N_i + q\,v_i\,p_i\,N^{-\beta} - q(D-1)\,(p_B\,v_B + p_C\,v_C)N^{-\beta-1}N_i. \tag{3}$$

The difficulty of the mathematical treatment lies in the dependence of the probabilities p_i on the individual number N_i. Using the relative densities $c_i = N_i/N$, $i = B, C$ of the species instead of their number, the competition dynamics is described by:

$$\frac{dc_B}{dt} = q\,(p_B\,v_B\,c_C - p_C\,v_C\,c_B)\,N^{-\beta-1}, \tag{4}$$

with $c_B + c_C = 1$. The temporal change of the densities is determined by the weighted relative difference in the densities and it depends in a nontrivial way on the fractal dimension. Detailed analysis of the above model demonstrated that coexistence is possible, giving as well, an exact condition for stable coexistence [8].

The theoretical results were confirmed by numerical simulations, which were performed, among others, in a frequently used model of chaotic flows, the flow in the wake of a cylindrical obstacle where the von Kármán vortex street is present. An explicit expression for the stream function was given in [35], which has been checked to be consistent with a Navier-Stokes simulation at fluid Reynolds number around 250. In what follows, for inertial simulations we will use the same flow model, which opens the possibility of direct comparison with the results in the passive case.

III. INERTIAL AND FINITE SIZE EFFECTS

The total force exerted on a small spherical particle of radius a and mass m_p immersed in a fluid is given by [30–32]:

$$F_i = m_f \frac{du_i}{dt} - \frac{m_f}{2}\left(\frac{dv_i}{dt} - \frac{du_i}{dt}\right) - 6\pi a\mu(v_i - u_i). \quad (5)$$

The first term on the right hand side represents the fluid force on the particle from the undisturbed flow field, where $\mathbf{u}$ is the velocity of the undisturbed flow and d/dt is the total hydrodynamical derivative following the fluid motion $du_i/dt = \partial u_i/\partial t + (\mathbf{u}\cdot\nabla)u_i$. The second term is the so called "added mass term", expressing the fact that an inertial particle brings into motion a certain amount of fluid, proportional to half of its volume, where m_f is the mass of the displaced fluid. The last term contains the Stokes drag, proportional to the difference between the particle velocity v_i and the flow velocity u_i, and vanishing for point-like tracers. An additional force contribution is the Boussinesq–Basset history integral term $-6\pi a^2\mu\int_0^t d\tau\{[d(v_i-u_i)]/d\tau\}/\sqrt{\pi\nu(t-\tau)}$, where μ and ν are the fluid's dynamic and kinematic viscosities, respectively. The history term is due to the fact that the particle modifies the flow locally. By assuming that the particle takes a long time to return to a fluid region visited earlier, this term can be neglected. Equation (5) is valid for initial tracer velocities approximately matching the fluid velocity.

The equations of motion $F_i = m_p dv_i/dt$ for an inertial tracer can be cast in the dimensionless form:

$$\frac{d\mathbf{v}}{dt} - \frac{3}{2}\,\mathcal{R}\,\frac{d\mathbf{u}}{dt} = -\mathcal{A}\,(\mathbf{v}-\mathbf{u})\,. \quad (6)$$

where the dimensionless variables are defined by: $\mathbf{r} \to L\mathbf{r}, \mathbf{v} \to U\mathbf{v}, \mathbf{u} \to U\mathbf{u}$, and $t \to (L/U)t$, where L is a typical large-scale length and U is a characteristic large-scale fluid velocity.

The two parameters are the "mass ratio parameter" $\mathcal{R}$ and the "inertia or size parameter" $\mathcal{A}$ given by

$$\mathcal{R} = \frac{2\rho_f}{\rho_f + 2\rho_p}, \quad (7)$$

$$\mathcal{A} = \mathcal{R}/St, \quad St = \frac{2}{9}\left(\frac{a}{L}\right)^2 Re, \quad (8)$$

where ρ_f and ρ_p are the densities of the fluid and of the particle, respectively, St is the particle Stokes number, and $Re = UL/\nu$ is the fluid Reynolds number. In the case of the von Kármán vortex street studied in this paper, the characteristic linear size of the flow L is the cylinder radius and it serves simultaneously as length unit. The period of the flow is taken as the time unit.

As a function of the mass ratio parameter we can distinguish three different regimes. For $\mathcal{R} = 2/3$ the particle has the same density as the fluid, and it is called *neutral tracer*. In the range where $0 < \mathcal{R} < 2/3$ the particles are heavier then the surrounding fluid and they are called *aerosols*. The $2 > \mathcal{R} > 2/3$ interval corresponds to the *bubble* regime. The ideal pointlike tracer can be reached in the $\mathcal{A} \to \infty$ limit.

Recent results in the field of inertial particle ensembles have shown that inertial effects can considerably modify the advection dynamics: changes in the escape rate from the chaotic set, changes in the residence time the particles spend in the wake, segregation of particles, appearance of attractors have been reported in the case of non interacting inertial particles [25]. Since the velocity $\mathbf{v}$ of the inertial particle is not determined merely by the spatial coordinates as it is in the passive case, and it differs generally from that of the flow $\mathbf{u}$, the inertial dynamics takes place in a 4–dimensional phase space: besides the two spatial coordinates x and y, the two velocity components v_x and v_y have to be taken into account. The invariant sets: the chaotic saddle responsible for the chaotic motion and its stable and unstable manifolds are four-dimensional objects.

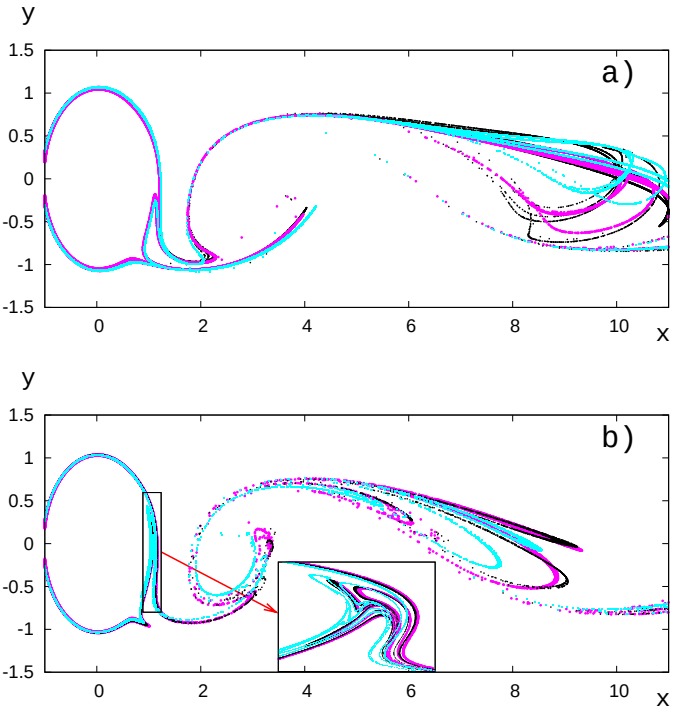

FIG. 1: Projection of the unstable manifold into the plane of the flow for different inertial particles obtained as in Ref [25]. (a) Aerosols for three different sets of parameters: $\mathcal{R}_B = 0.5$ and $\mathcal{A}_B = 30$ (grey–magenta online), $\mathcal{R}_C = 0.5$ and $\mathcal{A}_C = 20$ (black), $\mathcal{R}_D = 0.4$ and $\mathcal{A}_D = 30$ (light grey–cyan online). (b) Bubbles for three different sets of parameters: $\mathcal{R}_B = 0.8$ and $\mathcal{A}_B = 30$ (grey–magenta online), $\mathcal{R}_C = 0.8$ and $\mathcal{A}_C = 20$ (black), $\mathcal{R}_D = 1$ and $\mathcal{A}_D = 30$ (light grey–cyan online). The cylinder is situated in the origin. The magnification in the inset presents pictorially the interwoven fractal filaments of the different unstable manifolds.

From the point of view of the present paper, an es-

pecially important effect is that the unstable manifold of the inertial particles projected into the plane (x, y) of the flow, slightly deviates from the unstable manifold of the passive case. The deviation depends on the particles' size and density parameters (Fig. 1). Note that in the inertial dynamics the fractal support on which the competition takes place is only the 2–dimensional projection of the full unstable manifold into the configuration space (it is the spatial distribution of the species which determines the competition dynamics and not the particles' velocity). If competition between different inertial particle ensembles takes place on slightly shifted copies of the unstable manifold, then the strength of competition decreases because of partial spatial segregation: species have thus enhanced chance to survive and coexist.

IV. COEXISTENCE OF INERTIAL SPECIES

The possibility of enhanced coexistence suggested by Fig. 1 was checked in systematic numerical experiments. For the sake of convenience we carried out simulations on a uniform rectangular grid of lattice size ε covering both the incoming flow and the mixing region in the wake of the cylinder. Tracers are considered to be at the center of the cells. The projection of the tracer dynamics on a grid defines a mapping among the grid cells and particles are translated under the map with multiple integers of the lattice spacing ε. Initially, nearly all of the cells are occupied by component A, the resource material and only few cells contain species B and C (and later $D, E, ...$ in case of more than two competitors) competing for the same resource A. The interaction between the species is limited to the competition for the resource A, and it is assumed that they do not influence each other otherwise. Each iteration of the process consist of two consecutive mappings. The first mapping describes the advection of the particles on the grid over some time lag τ (chosen to be $\tau = 0.2$), while the second corresponds to the instantaneous reproduction occuring on the same grid of cells. If a cell contains B or C at the time of the reproduction, those from the 8 neighbouring cells which contain resource material A, get occupied by B or C, respectively. The birth rate of the species, therefore, is determined by the lattice size ε which can be seen as a reproduction range. In the following simulations ε is kept constant $\varepsilon = 1/200$. There is at most one individual in a cell. If two different species can reproduce to the same cell at the same time, it is chosen randomly which one will occupy the cell. When a cell gets occupied by a new individual, we suppose that the new particle takes over the instantaneous velocity of the flow in that cell. The death of the species with rate d_B, d_C, ... is also included in the model, and it takes place simultaneously with their reproduction. When an individual dies, its cell becomes occupied again by the resource material A, hence in a next reproduction step new particles can be created in that cell. Since the reproduction range is the same for all of the particles, the ratio between their death rates determines which of them should win the competition. Therefore, we use the death rate of the species as the parameter describing their fitness.

Initially we introduce a droplet of competitors in front of the cylinder. The outcome of the competition depends strongly on whether the initial droplet intersects with the stable manifold of the chaotic set. If the initial droplet is off x axis, it does not penetrate the mixing region in the wake of the cylinder, and the initial droplet is simply stretched before the whole amount of competitors is washed out downstream. Equations (1-4) are valid only for initial droplets overlapping with the stable manifold of the chaotic set. In the following we present results obtained by using two different types of initial setup. In both cases the initial droplet is situated in the region $[-2 : -1.8] \times [-0.1 : 0.1]$. In the first case the droplet is formed by two different species, which are distributed in two parallel stripes of the same length and width along the x axis, with one species above, the other below the axis. In the second case the full initial droplet is occupied by one of the species, and later (after some time delay Δt), from the same place, the next species enters the mixing region. For simulations with $n > 2$ species we have always used the second type of initial condition.

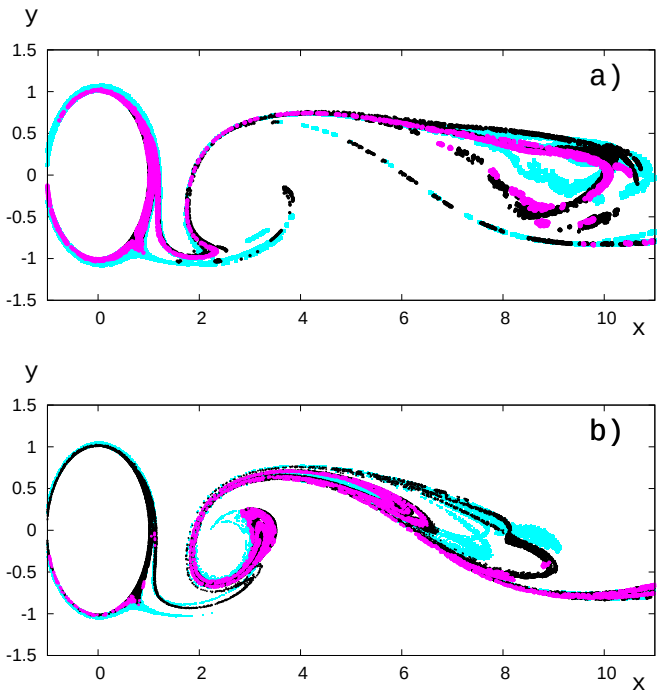

FIG. 2: Coexistence of three different inertial species from the aerosol (a) and the bubble (b) regime. The mass and size parameters and the corresponding colors are the same as in Figs. 1 a. and b. The death rates are: $d_B = 0.3$, $d_C = 0.24$, $d_D = 0.36$. The snapshot is taken after 30 time units. The initial condition is of second type with time delay $\Delta t = 0.2$.

Due to inertial effects the species have enhanced probability to coexist along the different unstable manifolds.

Such situations are presented in Figs. 2 a. and b. showing different inertial competitors in coexistence, the ones whose unstable manifolds have been shown in Fig. 1 without any competition.

The outer boundaries of the filaments covered by a given species extend according to an autocatalytic reproduction, the filaments touch and overlap each other, and they form narrow bands or patches. In the region $0 < x < 4$ where the chaotic saddle is located, the strong mixing stretches and folds the bands continuously, maintaining in this way the filamental features of the spatial distribution. Due to the enhanced perimeter of the bands, reproduction mainly takes place here. Downstream ($x > 6$), however, where the mixing is much weaker, the filaments overlap and the formation of patches is typical. Even though inside the patches individuals die and their place is occupied by resource material A, in the next step of reproduction the same species will fill in the cell, because no other species are present in the close vicinity.

To investigate the parameter dependence of the coexistence between two species B and C, we made a systematical study: by keeping fixed the death rate of B, $d_B = 0.3$, we changed the death rate of C from 0 to 1 and measured the relative density $c_C = N_C/(N_B + N_C)$ of species C after the steady state sets in in the system (after few tens of periods of the flow). We performed the same study for passive competitors as well. As expected, the parameter range in which coexistence is possible, increases considerably in comparison to the passive competition problem. In Fig. 3 we show the coexistence range for different size and inertia parameters of aerosols (a. and c.) and bubbles (b. and d.). For comparison to the passive case we plotted the passive coexistence curve in the background. Note that the condition of coexistence is $0 < c_C < 1$. Figures a. and b. correspond to competitors with small $\mathcal{A}$ parameters (relatively large particles), where the effect of inertia on coexistence is large. For large values of $\mathcal{A}$, associated with particle sizes on the order of the size of phytoplankton (see Discussion), coexistence remains, though in a smaller parameter range (Figs. 3 c. and d.). It is worth also noting that inertial coexistence in the case of panel (c) extends to nearly $d_C = 0$ since c_C is not exactly one, implying that a finite number of B species are alive.

First we discuss briefly a basic effect underlying the results appearing in Fig. 3. The decay is due to the biological death of the species characterized by the death rate, and the exponential escape from the chaotic set characterized by the escape rate. Earlier works regarding inertial particles have shown that aerosols escape the wake faster [25] because a centrifugal force acts on each particle moving along a closed (curvilinear) trajectory. This force is pushing the particles outwards, intensifying in this way their escape from the wake. In the case of bubbles an anti-centrifugal force is exerted on the particles, keeping them together for long time and slowing down the escape. This effect results in a broader coexistence range for bubbles than for aerosols, cf. the left and right panels of Fig. 3.

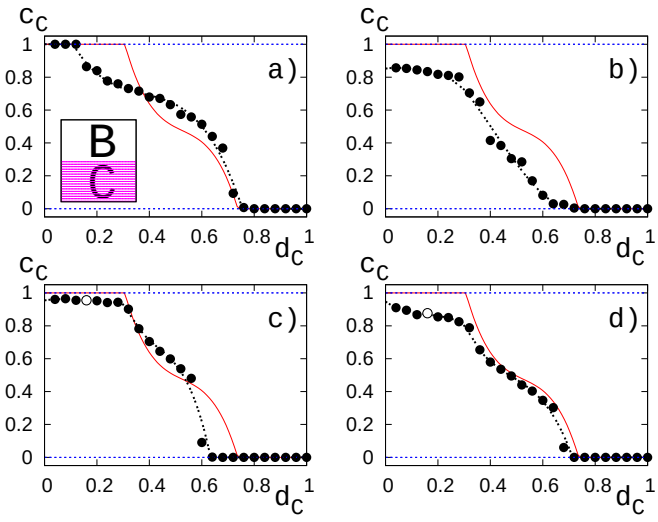

FIG. 3: Competition between two inertial species: relative density of species C as a function of their death rate d_C. The dotted curve is a line fitted to the numerical results (bulk circles). The course of reaction starts with an initial droplet situated at $[-2 : -1.8] \times [-0.1 : 0.1]$ in front of the cylinder. Inside this droplet species B and C are distributed in two parallel horizontal stripes as indicated in the inset. The death rate of species B is fixed at $d_B = 0.3$. a) aerosols: $\mathcal{R}_B = 0.5$, $\mathcal{R}_C = 0.4$, $\mathcal{A}_B = 30$, $\mathcal{A}_C = 20$, b) bubbles: $\mathcal{R}_B = 0.8$, $\mathcal{R}_C = 1$, $\mathcal{A}_B = 30$, $\mathcal{A}_C = 20$, c) aerosols: $\mathcal{R}_B = 0.5$, $\mathcal{R}_C = 0.5$, $\mathcal{A}_B = 300$, $\mathcal{A}_C = 3000$, d) bubbles: $\mathcal{R}_B = 0.8$, $\mathcal{R}_C = 0.8$, $\mathcal{A}_B = 300$, $\mathcal{A}_C = 3000$. The passive coexistence curve is shown in the background with continuous thin line.

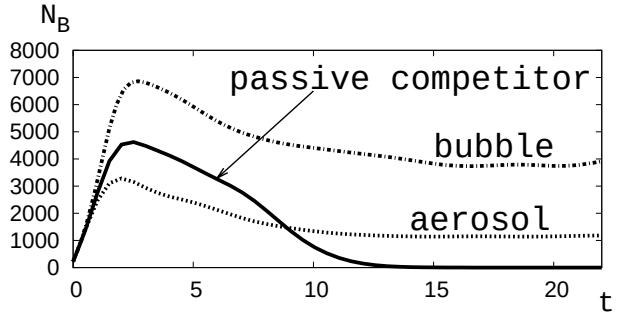

FIG. 4: Time evolution of the individual number of species B from three different inertial regimes: passive tracers (continuous line), aerosols with $\mathcal{R}_B = 0.5$, $\mathcal{A}_B = 300$ (dotted line) and bubbles $\mathcal{R}_B = 0.8$, $\mathcal{A}_B = 300$ (dash-dotted lines). In each case the death rate is $d_B = 0.3$ for the species shown, and $d_C = 0.16$ for the other competitor (not shown here).

For a better visualisation we compare how the number of competitors B evolves in time in different inertial regimes: Figure 4 makes clear that in the bubble regime the small escape rate results in a huge number of individuals and an accordingly big chance for persistence,

while in the aerosol regime the number of the individuals is smaller. After 15 time units a steady state sets in and the passive species is outcompeted, while the inertial competitor survives. We emphasize that in Fig. 4 we show only the weaker competitors from three different competition scenarios (for the points represented by empty circles in Figs. 3 c and 3 d).

Turning back to Figs. 3 c. and 3 d. we have to remark that a value of $\mathcal{A}_C = 3000$ is in the numerical simulations very close to the limit of pointlike tracers, and a further increase of the size parameter $\mathcal{A}$ would not have any observable effect in the simulations. The reason is that at such big values of $\mathcal{A}$, the split of the unstable manifolds is so small that it cannot be resolved with the resolution applied. Refining the resolution requires unreasonably huge computer time and memory consumption. In real aquatic systems, however, (the realistic size parameters $\mathcal{A}$ for plankton are a few thousands – see Discussion) any deviation of the unstable manifold greater than the size of the plankton is expected to be observable and this effect can contribute to their coexistence.

The fate of the populations is strongly influenced by the position of the initial droplet even in cases when it intersects the stable manifold of the chaotic set. To demonstrate the sensitivity of the competition on the initial conditions, in Fig. 5 we show the coexistence of the same aerosols as in Fig. 3 c. with the only change that their initial positions are interchanged. The coexistence curve changes both in the passive and the inertial case but the fact that the inertia of the particles increases the coexistence range remains valid regardless of the initial setup.

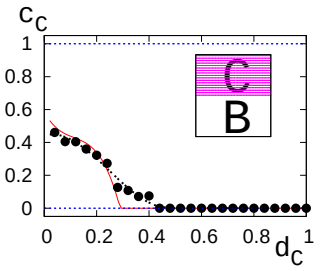

FIG. 5: The same as in Fig. 3 c. but the initial positions of species B and C are interchanged (inset). The outcome of the competition is drastically changed, but also in this case the coexistence range is increased by inertial effects.The passive coexistence curve is shown in the background with continuous thin line.

To reflect reality better, where the species come continuously from other regions or appear from upwellings of water, we assume that the species B and C start from the same spatial position (the square specified in the caption to Fig. 3), but with some time delay Δt after each other. In the numerical simulation we choose a time delay $\Delta t = \tau = 0.2$ equal to the time lag between reproductions, meaning that the second species enters the mixing region at the time of the first reproduction of the first species. The outcome of the competition with this setup is shown in Fig. 6. The initial time instant when the different species enter the mixing region can influence the competition scenario because the outcome of the competition depends on the degree of overlap of the initial droplet with the continuously moving stable manifold. Additional simulations have shown that the coexistence curves change if we choose another time delay Δt or we interchange the starting time of the different species (Fig. 7), but the increased coexistence range as compared to the passive case remains valid. Coexistence of the species is in general more pronounced than in the case of the previously used initial distribution of the competitors (Figs.3 and 5).

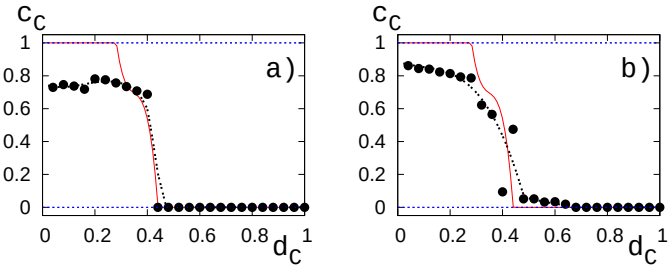

FIG. 6: The same as in Fig. 3 a. and b. but the initial droplet is of second type with time delay $\Delta t = 0.2$. The relative density of species is measured after 70 time units.

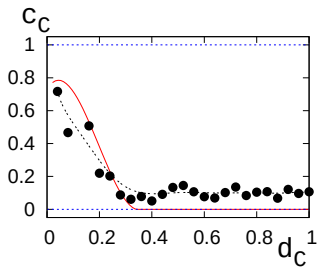

FIG. 7: The same as in Fig. 6 a. but the starting time of the species B and C are interchanged. Also in this case the coexistence range is increased by inertial effects. The passive coexistence curve is shown in the background with continuous thin line.

As stated before, the shift of the unstable manifold opens, in principle, the possibility for infinitely many species to coexist. This has been demonstrated for three species at a single set of parameters in Fig. 2. Now we study the robustness of coexistence for three and five competing species in Figs. 8 and 9, respectively, by changing the death rate of one of the species. The outcome of the competition usually fluctuates wildly, but there are definite intervals of death rates where three or five species remain in coexistence.

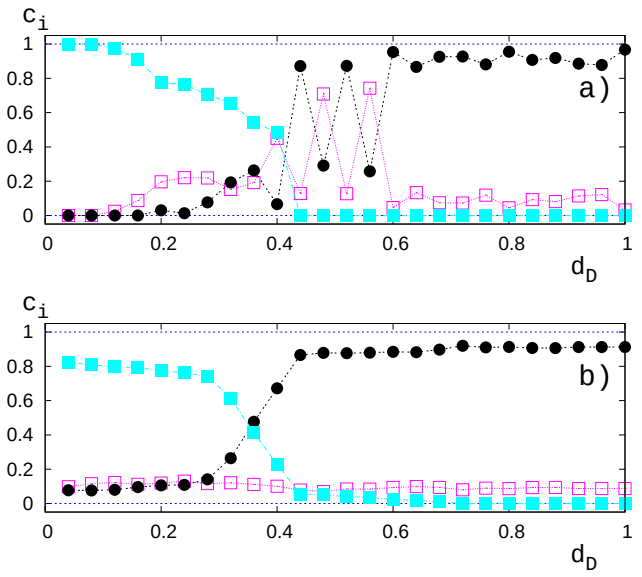

FIG. 8: Competition between three inertial species: relative densities $c_i = N_i/(\Sigma N_i)$ of species $i = B$ (empty squares), $i = C$ (bulk circles), $i = D$ (bulk squares), as a function of the death rate of species D. The initial droplet starts from the same position as in Fig. 6, the different species start with a time delay $\Delta t = 0.2$ one after the other. The death rates of species B and C are fixed to the values $d_B = 0.3$ and $d_C = 0.24$. The parameters are: (a) aerosols $\mathcal{R}_\mathcal{B} = 0.5$, $\mathcal{A}_\mathcal{B} = 30$, $\mathcal{R}_\mathcal{C} = 0.5$, $\mathcal{A}_\mathcal{C} = 20$, $\mathcal{R}_\mathcal{D} = 0.4$, $\mathcal{A}_\mathcal{D} = 30$, (b) bubbles $\mathcal{R}_\mathcal{B} = 0.8$, $\mathcal{A}_\mathcal{B} = 30$, $\mathcal{R}_\mathcal{C} = 0.8$, $\mathcal{A}_\mathcal{C} = 20$, $\mathcal{R}_\mathcal{D} = 1$, $\mathcal{A}_\mathcal{D} = 30$.

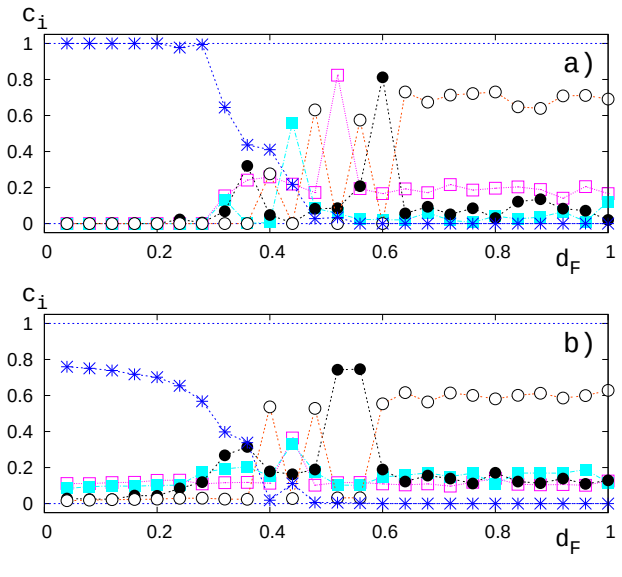

FIG. 9: Competition between five inertial species: relative densities $c_i = N_i/(\Sigma N_i)$ of species $i = B$ (empty squares), $i = C$ (bulk circles), $i = D$ (bulk squares), $i = E$ (empty circles), $i = F$ (stars), as a function of the death rate of species F. The initial droplet starts from the same position as in Fig. 6, the five different species start with a time delay $\Delta t = 0.2$ one after the other. The death rates of species B, C, D, and E are fixed to the values $d_B = 0.3$, $d_C = 0.24$, $d_D = 0.20$, and $d_E = 0.28$, respectively. The parameters are: (a) aerosols: $\mathcal{R}_B = 0.5$, $\mathcal{A}_B = 30$, $\mathcal{R}_C = 0.5$, $\mathcal{A}_C = 20$, $\mathcal{R}_D = 0.4$, $\mathcal{A}_D = 30$, $\mathcal{R}_E = 0.4$, $\mathcal{A}_E = 20$, $\mathcal{R}_F = 0.6$, $\mathcal{A}_F = 30$, and (b) bubbles: $\mathcal{R}_B = 0.8$, $\mathcal{A}_B = 30$, $\mathcal{R}_C = 0.8$, $\mathcal{A}_C = 20$, $\mathcal{R}_D = 1$, $\mathcal{A}_D = 30$, $\mathcal{R}_E = 1$, $\mathcal{A}_E = 20$, $\mathcal{R}_F = 1.1$, $\mathcal{A}_F = 30$.

V. DISCUSSION

Inertia can be understood as a kind of "activity" of the particles. The initial assumption is very simple, we just take into account that the tracers have small but finite size, and they follow the motion of the fluid with some inertia, but the impact of inertia on the particle dynamics is remarkable.

The aim of the present work has been to bring into focus this kind of activity. As an example of biological relevance we have chosen the problem of competition between species. It has been shown earlier that two passively advected species competing for a single material can coexist in open chaotic flows, but inertial and finite size effects have not been previously taken into account.

The main idea of the paper is that due to inertial and finite size effects, the different inertial species accumulate along slightly different unstable manifolds. In this way, the strength of the competition between the inertial species decreases as compared to the passive competitors. Coexistence of the "inertial" populations is a more robust phenomenon than that of the passive species. One important result is that inertia and finite size of the particles increase the parameter range where coexistence is present independently of the fact whether the species are more or less dense than the water. Coexistence was observed in a wide range of size (from $\mathcal{A} = 20$ to $\mathcal{A} = 3000$). Note, that the dimensionless size parameter defined by Eq. (8) with the values $\nu = 10^{-6}\ m^2/s$, as the kinematic viscosity of water, $a = 200\mu m$ as the plankton size, and $\mathcal{R} = 0.6$ as the density parameter, gives $\mathcal{A} \approx 60L/U$. Taking the typical length scale $L = 10m$ and the characteristic velocity $U = 0.1\ m/s$, we obtain $\mathcal{A}$ approximately a few thousands.

The most important result of the paper is that it gives an explanation why a large number of different species competing for a few resource is able to coexist in chaotic flows. In conclusion, the "hydrodynamical explanation" of the plankton paradox becomes more plausible if inertia and the finite size of the competitors are taken into account.

The problem presented in the paper is just one example showing the importance of inertial effects in the advection dynamics, but inertia is expected to play a significant role also in other advection–reaction systems where the biological interaction between species is of other type (prey–predator systems, models of prebiotic evolution, etc.).

Acknowledgement

We are grateful to H. Kantz for making possible reciprocal visits of the coauthors, and for his hospitality at the Max Planck Institute for the Physics of Complex Systems, Dresden. The support of the Hungarian Science Foundation (OTKA Nos T037726, T047233, TS044839, F042476) is also acknowledged. Gy. K. was supported by a Bolyai grant.

[1] G.E. Hutchinson, Am. Nat. **95**, 137 (1961).
[2] G.F. Gause and A.A. Witt, Am. Nat. **69**, 596 (1935).
[3] G. Hardin, Science **131**, 1292 (1960).
[4] J.B. Wilson, N. Z. J. Ecol. **43**, 17 (1990).
[5] P. Chesson, Annu. Rev. Ecol. Syst. **31**, 343 (2000).
[6] I. Scheuring et al., Freshwater Biology **45**, 123 (2000).
[7] G. Károlyi et al.. PNAS **97**, 13661 (2000).
[8] I. Scheuring et al., Theor. Pop. Biol. **63**, 77 (2003).
[9] T. Tél et al., Phys. Rep. **413**, Nos. 2-3 (2005).
[10] Z. Toroczkai et al., Phys. Rev. Lett. **80**, 500 (1998).
[11] G. Károlyi et al., Phys. Rev. E **59**, 5468 (1999).
[12] W.A. Sirignano, ASME J. FLuids. Eng. **115**, 345 (1993).
[13] P. Tanga, A. Provenzale, Physica **D76**, 202 (1994);
[14] D.E. Stock, ASME J. FLuids. Eng. **118**, 4 (1996).
[15] T. Elperin, N. Kleeorin and I. Rogachevskii, Phys. Rev. Lett. **77**, 5373 (1996).
[16] E.E. Michaelides, J. Fluids. Eng. **119**, 233 (1997).
[17] A. Bracco et al, Phys. Fluids **11**, 2280 (1999).
[18] A. Babiano et al, Phys. Rev. Lett. **84**, 5764 (2000).
[19] T. Nishikawa, Z. Toroczkai, and C. Grebogi, Phys. Rev. Lett. **87**, 038301 (2000); T. Nishikawa et al,. Phys. Rev. E **65**, 026216 (2002).
[20] E. Balkovsky, G. Falkovich, and A. Fouxon, Phys. Rev. Lett. **86**, 2790 (2001).
[21] T. Shinbrot et al, Phys. Rev. Lett. **86**, 1207 (2001).
[22] R. Reigada, F. Sagues and J. M. Sancho, Phys. Rev. E. **64**, 026307 (2001).
[23] C. Lopez, Phys. Rev. E. **66**, 027202 (2002).
[24] J. H. E. Cartwright, M. O. Magnasco, O. Piro, Phys. Rev. E **65**, 045203 (2002).
[25] I.J. Benczik, Z. Toroczkai, and T. Tél, Phys. Rev. Lett. **89**, 164501 (2002); I.J. Benczik, Z. Toroczkai, and T.Tél, Phys. Rev. E **67**, 036303 (2003).
[26] A.E. Motter, Y.C. Lai, and C. Grebogi, Phys. Rev. E **68**, 056307 (2003).
[27] Y. Do and Y.C. Lai, Phys. Rev. Lett. **91**, 224101 (2003); Y. Do and Y.C. Lai, Phys. Rev. E **70**, 036203 (2004).
[28] C. Lopez and A. Puglisi, Phys.Rev. E **69**, 046306 (2004).
[29] T. Tél et al., Chaos **14**, 72 (2004).
[30] M.R. Maxey and J.J. Riley, Phys. Fluids **26**, 883 (1983).
[31] M.R. Maxey, Phys. Fluids **30**, 1915 (1987).
[32] T.R. Auton et al., J. Fluid. Mech. **197**, 241 (1988).
[33] R. E. Lee, *Phycology*, Cambridge University Press, Cambridge (1999).
[34] W.S.C. Gurney and R.M. Nisbet, *Ecological Dynamics*, Oxford University Press, Oxford (1998).
[35] C. Jung, T. Tél, and E. Ziemniak, Chaos **3**, 555 (1993).